Journal of Power Sources 189 (2009) 288–296

Contents lists available at ScienceDirect

Journal of Power Sources

journal homepage: www.elsevier.com/locate/jpowsour

A short review on surface chemical aspects of Li batteries: A key for a good performance

S.K. Martha[a], E. Markevich[a], V. Burgel[a], G. Salitra[a], E. Zinigrad[a], B. Markovsky[a], H. Sclar[a], Z. Pramovich[a], O. Heik[a], D. Aurbach[a,*], I. Exnar[b], H. Buqa[b], T. Drezen[b], G. Semrau[c], M. Schmidt[c], D. Kovacheva[d], N. Saliyski[d]

[a] Department of Chemistry, Bar-Ilan University, Ramat-Gan 52900, Israel
[b] HPL, SA PSE-B, EPFL 1015 Lausanne, Switzerland
[c] Merck KGaA, Frankfurter Str. 250, D 64293 Darmstadt, Germany
[d] Institute of General and Inorganic Chemistry, Bulgarian Academy of Sciences, Sofia 1113, Bulgaria

ARTICLE INFO

Article history:
Received 30 July 2008
Accepted 12 September 2008
Available online 2 October 2008

Keywords:
Li battery
Ionic liquid
Cathode
Surface chemistry
$LiMnPO_4$
Transition metal oxide

ABSTRACT

We review herein several important aspects of surface chemistry in Li-ion batteries, and discuss the use of ionic liquids (ILs) for rechargeable Li batteries. We explored the suitability of ILs for 5 V cathodes and Li-graphite anodes. Some advantages of the use of ILs to attenuate the thermal behavior of delithiated cathode materials are demonstrated. We also report briefly on a comparative study of the following cathode materials: $LiNi_{0.5}Mn_{0.5}O_2$; $LiNi_{0.33}Mn_{0.33}Co_{0.33}O_2$; $LiNi_{0.4}Mn_{0.4}Co_{0.2}O_2$; $LiNi_{0.8}Co_{0.15}Al_{0.05}O_2$ and $LiMnPO_4$, in standard electrolyte solutions based on mixtures of alkyl carbonates and $LiPF_6$. We also discuss aging, rate capability, cycle life and surface chemistry of these cathode materials. The techniques applied included electrochemical measurements, e.g., XRD, HRTEM, Raman spectroscopy, XPS and FTIR spectroscopy. We found that ILs based on cyclic quaternary alkyl ammonium cations may provide much better electrolyte solutions for 5 V cathodes than standard electrolyte solutions, while being quite suitable for Li-graphite electrodes. All the lithiated transition metal oxides studied (as mentioned above) develop unique surface chemistry during aging and cycling due to the acid-base and nucleophilic reactions of their surface oxygen anions. $LiMn_{0.33}Ni_{0.33}Co_{0.33}O_2$ has the highest rate capability compared to all the other above-mentioned cathode materials. Cathodes comprising nanometric size carbon-coated $LiMnPO_4$ produced by HPL demonstrate a better rate capability than $LiNi_{0.5}Mn_{0.5}O_2$ and $LiNi_{0.8}Co_{0.15}Al_{0.05}O_2$ cathodes. The former material seems to be the least surface reactive with alkyl carbonates/$LiPF_6$ solutions, among all the cathode materials explored herein.

1. Introduction

All the relevant electrodes for Li-ion batteries, excluding 1.5 V systems such as lithiated titanium oxide (L—T—O), are surface film controlled (SFC) systems because they develop rich surface chemistry that determines their charge transfer behavior. On the anode side, all conventional electrolyte systems can be reduced in the presence of Li ions below 1.5 V, thus forming insoluble Li compounds [1]. These may include Li_2O, LiOH, LiF, LiCl, Li_xPF_y, Li_xPOF_y, ROLi, $ROCO_2Li$, RCOOLi, and polymeric species. Due to the unique properties of Li—O, Li—X (halide), Li—S, Li—N, and Li—C bonds and related ionic compounds, all thin films comprising Li salts can transport Li ions under an electrical field, even if they are thick enough to block any electron transport through them (between reductive electrodes such as Li, Li-graphite, Li–Si and other Li alloys and solution species). Hence, Li, Li-graphite or Li alloy electrodes are always passivated in polar aprotic electrolyte solutions and by Li-ion conducting surface films that behave like a solid electrolyte interphase (the SEI model) [2].

The cathode side is less trivial. It should be noted that alkyl carbonates can be oxidized at potentials below 4 V vs. Li/Li^+ [3]. However, these reactions are inhibited by passivated Al current collectors and by the composite cathodes. It should be emphasized that aluminum, which is an active metal, can be used as a current collector because it is fully passivated by Al_2O_3 and AlF_3 in $LiPF_6$/alkyl carbonate solutions [4]. The lithiated transition metal cathodes may also develop very rich surface reactions. In their lithiated state, nucleophilic surface oxygen anions attack electrophilic RO(CO)OR, thus forming surface $ROCO_2Li$, $ROCO_2M$, ROLi, ROM, etc. [5].

* Corresponding author. Tel.: +972 3 5218317; fax: +972 3 7384053.
E-mail address: aurbach@mail.biu.ac.il (D. Aurbach).

0378-7753/$ – see front matter © 2008 Elsevier B.V. All rights reserved.
doi:10.1016/j.jpowsour.2008.09.084

In their delithiated state, when high potentials are reached, the polymerization of solvent molecules such as EC by cationic stimulation forms polycarbonates on the cathode particles' surface. Another surface phenomenon of cathodes comprising spinel type or layered Li_xMO_y materials is the dissolution of transition metal cations during cycling and aging [6]. This change in stoichiometry forms surface-inactive phases. Hence, upon the aging of the electrodes' (Li_xMO_y) particles in standard electrolyte solutions, they develop a core–shell structure in which the outer part may contain, in addition to the above-mentioned surface reaction products, lithium and/or transition metal deficient (Li_zMO_k) species of different stoichiometry, as compared to the active mass [7]. It should be emphasized that the dissolution of transition metal ions from the cathodes in Li-ion batteries is a detrimental phenomenon because these metal ions are reduced on the anode side, thus forming metallic clusters that destroy the passivation of carbonaceous and Li anodes [8].

It was also possible to detect red-ox reactions between Li_xMO_y (lithiated transition metal oxides) and solution species that form CO_2 as a product and inactive $LiMO_y$ with the transition metal, M, at a lower oxidation state. Of significant influence are the acid-base reactions which occur in $LiPF_6$ solutions (e.g., with HF), and which are inevitable. A very good example is the commonly-used cathode material $LiCoO_2$, which may have a rich surface chemistry that influences its performance in standard electrolyte solutions. We detected the following reaction [9]:

$$4LiCo^{III}O_2 \rightarrow Co^{IV}O_2 + Co^{III}Co^{IV}{}_2O_4 + 2Li_2O,$$

which is in fact a disproportionation of $LiCoO_2$. This reaction is driven by the following reaction:

$$Li_2O + 2HF \rightarrow 2LiF + H_2O.$$

We also found that the thus formed/existing Co^{IV} compounds oxidize alkyl carbonate solvent molecules, thus forming CO_2 [9]. When $LiCoO_2$ is transformed to Co compounds (e.g., Co_3O_4), the bivalent Co^{2+} ions can relatively easily dissolve in solutions. We unambiguously found that the presence of Co^{2+} in standard solutions stabilized $LiCoO_2$ cathodes and enables their very good operation, even at elevated temperatures (up to 80 °C, measured) [10]. In fact, the dissolution of Co^{2+} could not be a problem in real battery systems where the electrode mass-solution volume ratio is high, and hence saturation of the solutions with Co^{2+} ions can be easily reached. However, the Co^{2+} ions migrate to the anode side, Li or Li–carbon electrodes, and are reduced there to Co metal clusters. The presence of these metallic clusters in the surface films of the anode destroys its passivation, probably because it extends the range of electron transfer (tunneling) from the active anode material to solution species, despite its passivation by surface films [10]. The consequence of this are extensive surface reactions on the anode side (reduction of solution species), which increased pronouncedly the impedance of the anode side in the cell. Thus, transition metal ion dissolution in Li-ion batteries should be avoided.

It is important to note that in contrast to bulk studies where the judicious use of diffraction and electron microscopy techniques can provide precise structural and crystallographic analysis, the surface analysis of all the electrode materials relevant to Li-ion batteries can not provide really truly unambiguous results. Thin films with a mosaic-type structure, which contain several different components, cannot be precisely probed by any of the surface sensitive techniques that we have. Moreover, the surface chemistry of all these systems is strongly influenced by additives and contaminants that can occasionally be present in solutions. Thereby, similar surface studies in different labs can provide diverse results due to the different level of contaminants in the electrolyte solutions used.

This paper and related work are aimed at advancing the understanding of the complicated surface chemistry of Li battery systems. We focus on two main subjects:

1. Ionic liquids (ILs) and their suitability for Li in battery systems.
2. The surface chemistry of novel cathode materials for Li-ion batteries.

ILs may be important electrolyte systems or additives for Li batteries because of their wide potential window and promising safety features (low volatility and flammability as compared to standard solutions, better thermal stability). As regards the second topic, we focus on a comparative study that includes novel cathode materials: $LiNi_{0.5}Mn_{0.5}O_2$, $LiNi_{0.33}Mn_{0.33}Co_{0.33}O_2$, (NMC) $LiNi_{0.4}Mn_{0.4}Co_{0.2}O_2$ (a layered structure), produced by a self-combustion reaction (SCR) including both nano- and micro-particles, and nano $LiMnPO_4$. For comparison, we also studied commercial $LiNo_{0.8}Co_{0.15}Al_{0.05}O_2$ (NCA) cathode material. The results thus obtained could be compared with the results of previous studies with more conventional systems: $LiCoO_2$ and $LiFePO_4$. We used surface sensitive techniques such as FTIR, XPS and microRaman spectroscopy, XRD and high resolution electron microscopy in conjunction with standard electrochemical techniques. Special efforts were devoted to the surface chemical studies of the above systems.

2. Experimental

2.1. Materials

Synthetic graphite samples (Timrex, Inc.) and natural graphite powders NG-15 (Kansai Coke and Chemicals, Inc.) were used. 1-methyl-1-propylpiperidinium bis(trifluoromethylsufonyl)imide (MPPpTFSI) (>99%) was purchased from Toyo Gosei Co., Ltd. (Japan). The water content in the IL was determined as less than 7 ppm by Karl Fischer titration. All other ionic liquids related to this study were obtained from Merck KGaA, Germany. Lithium bis(trifluoromethylsulfonyl)imide (LiTFSI) (99.95%) was obtained from Aldrich. Standard electrolyte solutions (EC-DMC/$LiPF_6$) were purchased from Tomiyama (Japan) and could be used as received. Nanometric carbon-coated $LiMnPO_4$ powder, produced by the polyol method, was obtained from HPL (Switzerland), $LiNi_{0.8}Co_{0.15}Al_{0.05}O_2$ was obtained from Toda (Japan) $LiNi_{0.5}Mn_{0.5}O_2$, $LiNi_{0.33}Mn_{0.33}Co_{0.33}O_2$ and $LiNi_{0.4}Mn_{0.4}Co_{0.2}O_2$ were produced by a self-combustion reaction from the metal nitrates in the right stoichiometry and sucrose as a fuel, as described elsewhere [11]. Further calcination of the as-prepared lithiated metal oxide in air to 700–900 °C produced the layered materials as nano-sized, submicron or micrometric particles, depending on the temperature (in this range) and duration of annealing. XRD patterns of all the materials we worked with, confirmed that we indeed obtained the right materials. HRTEM measurements (atomic resolution) provided nice images of the layered structures. The average surface area (BET method) of the nano, submicron and micronic powders was usually 7–8, 3–5, and 2 $m^2\,g^{-1}$, respectively.

2.2. Electrodes, cells and electrochemical measurements

Composite electrodes containing the active mass, carbon black and binder (usually PVdF from Solvey) were prepared, as already described [12]. For the anodes (graphite) and cathodes the current collectors were copper and aluminum foils, respectively, and the active mass was 90% and 80%, respectively. We used two- or

three-electrode cells for the electrochemical tests in which lithium foil served as counter and reference electrodes. The configuration was coin-type cells (2032, NRC Canada). The electrochemical measurements included slow and fast scan rate cyclic voltammetry and chronopotentiometry (galvanostatic cycling) and were carried out using equipment from Maccor, Arbin (computerized multichannel analyzers for galvanostatic cycling) and Solartron (an eight channel electrochemical analyzer, model BTU-1470). The electrochemical cells were composed under highly pure and controlled argon atmosphere in glove boxes from M Braun and VAC Inc.

2.3. Surface spectroscopic measurements

Raman spectra were measured in a back scattering configuration using a microRaman spectrometer HR 800 (Jobin Yvon Horiba, France), with He–Ne laser (excitation line 632.8 nm) and a microscope objective (x50, Olympus MPlan, 0.4 mm working distance, numerical aperture 0.75). FTIR spectra were measured using a Nicolet Magna 560 spectrometer placed in a glove box, with a diffuse reflectance accessory from Pike Technologies. FTIR spectra of pristine and aged composite electrodes were measured using a diffuse reflectance mode. We also measured the spectra of Li surfaces prepared in ethereal $LiN(SO_2CF_3)_2$ (Li-TFSI) solutions by cutting Li discs from a Li rod in solution, followed by *ex situ* reflectance measurements using the same above accessory (Li surfaces protected by NaCl windows, as already described [13]). XPS measurements of pristine and aged composite electrodes and of Li surfaces were carried out using a Kratos H Axis (England) spectrometer. We used a home-made transfer system that includes a gate valve and a magnetic manipulator for the transfer of the highly sensitive samples from the glove boxes (highly pure argon atmosphere) to the XPS system.

2.4. Structural analysis

XRD patterns of the electrode materials were obtained using a BRUKER-AXS, D8-Advance diffractometer. The electrode materials were also measured by HRTEM, including electron diffraction (JEOL-JEM-2011 200 kV). The surface area of the powders was measured by analyzing nitrogen adsorption according to the BET method (Gemini 2375, Micromeritics Inc., multipoint mode). The elements ratio in the cathode materials and the possible dissolution of transition metal cations in solutions during aging was measured by ICP (a system from Jobin Yvon Horiba, France).

2.5. Thermal analysis

The possibility of using ILs as additives for attenuating the thermal reactivity of delithiated cathodes (e.g., $Li_{0.5}CoO_2$) in standard electrolyte solutions was carried out using DSC (Model DSC 822 Mettler Toledo Inc.) measurements of mixtures of powders scraped from delithiated $LiCoO_2$ cathodes and electrolyte solutions, hermetically sealed in the appropriate crucibles from the same company.

3. Results and discussion

3.1. On the possible use of ILs in rechargeable Li-ion batteries

As was already demonstrated [14], the use of ILs in Li-ion batteries can extend the electrochemical window of the electrolyte solutions beyond 5 V. However, it is questionable as to what extent the use of ILs can actually improve the safety features of Li-ion batteries, compared to standard electrolyte systems, i.e., alkyl

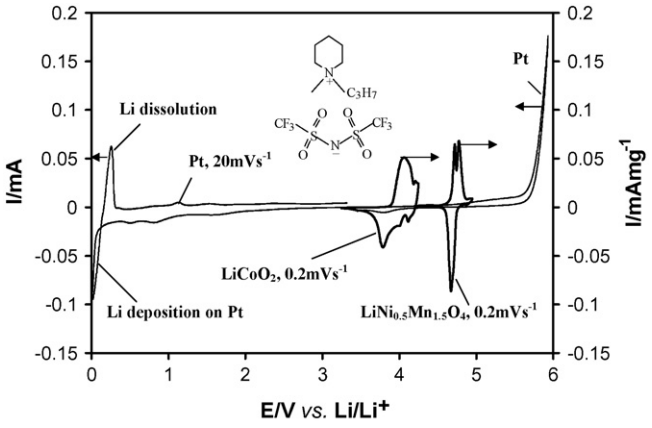

Fig. 1. The electrochemical stability window of 0.5 M LiTFSI in a MPPpTFSI electrolyte solution measured on a Pt electrode and cyclic voltammograms of $LiCoO_2$ and $LiNi_{0.5}Mn_{1.5}O_4$ spinel electrodes, as indicated. The relevant potential scan rates are also indicated.

carbonates and $LiPF_6$. Fig. 1 demonstrated the typical wide electrochemical window of an ionic liquid solution based on quaternary alkyl ammonium cations (propyl-methyl piperidinium in this case), a TFSI ($(CF_3SO_2)_2N^-$) anion, and LiTFSI. The figure demonstrates a reversible Li deposition/dissolution on platinum at low potentials and the pronounced anodic stability of these systems (>5.5 V vs. Li/Li^+) that fits nicely for all relevant cathode materials for Li-ion batteries. Typical CVs of $LiCoO_2$ and $LiMn_{1.5}Ni_{0.5}O_4$, as indicated, were added to the voltammetric presentation in Fig. 1 for this demonstration. The CV of $LiCoO_2$ reflects the well-known reversible lithiation/delithiation of 1/2 Li per $LiCoO_2$ via a first order phase transition [15] and the CV of the $LiMn_{1.5}Ni_{0.5}O_4$ reflects reversible lithiation/delithiation of one Li per formula in two consecutive phase transition steps, in which the Ni atoms change their oxidation state from 2^+ to 4^+ (via intermediate Ni^{3+}) [16]. The cathodic behavior of IL solutions and possible passivation phenomena of electrodes polarized to low potentials in IL solutions deserves special attention and discussion. We have already explored the cathodic behavior of tetraalkyl ammonium salts in polar aprotic solutions [17]. Such processes were also investigated by others [18]. For instance, Bu_4N^+ ($Bu = C_4H_9^-$) is reduced at potentials around 0 V (Li/Li^+) to Bu_3N,

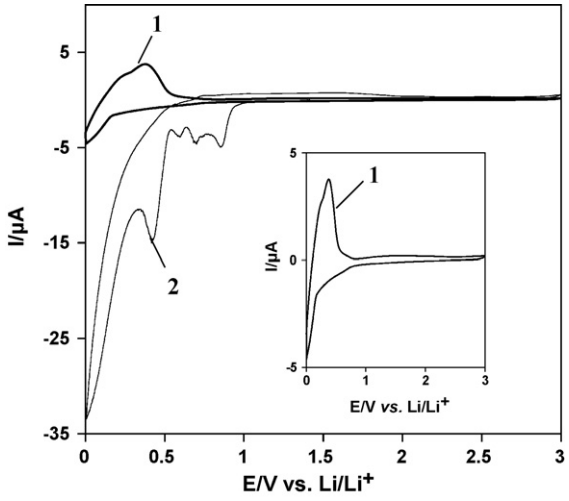

Fig. 2. Cyclic voltammograms measured with composite graphite electrodes (natural graphite flakes). (1) In a 1 M LiTFSI/MPPpTFSI solution, and (2) in Li salt free MPPpTFSI ionic liquid at scan rate 90 $\mu V s^{-1}$. Inset is an enlarged image of the CV (1).

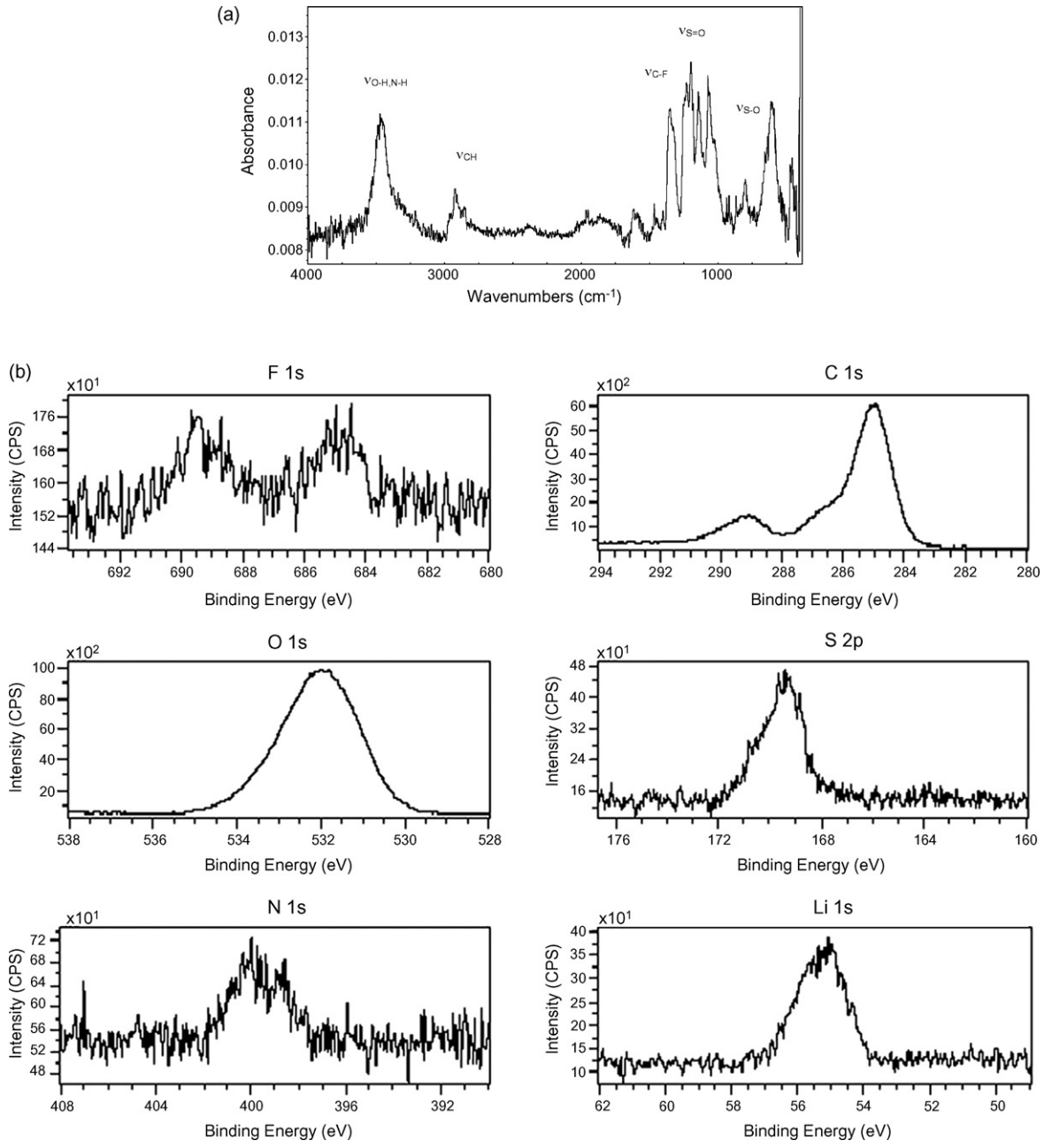

Fig. 3. (a) FTIR spectrum measured *ex situ* from a lithium metal surface freshly prepared and stored for a short period of time (2 min) in a dioxolane/LiTFSI 1 M solution. (b) O_{1S}, N_{1S}, C_{1S}, S_{2P}, and Li_{1S} XPS spectra measured from a Li metal surface, freshly prepared and stored for a short period of time in a dioxolane/LiTFSI 1 M solution.

butane and butene (i.e. Bu radicals are formed and undergo disproportionation). Hence reduction of R_4N^+ cations does not form surface species that can passivate electrodes. The presence of Li ions changes the picture completely. Most of the polar aprotic solvents and the relevant (big) anions (e.g., MX_y^-, X = halide, oxide; M = B, Cl, As, P, etc.) are reduced in the presence of Li ions on noble metal and carbonaceous electrodes to insoluble Li salts that can precipitate and passivate the electrode.

The reduction potential (Er) of R_4N^+ cations depends on the alkyl group, (e.g., Er is lower as the alkyl group is more bulky, and therefore $Er_{Bu} < Er_{Et} < Er_{Me}$). Hence, the cathodic behavior of ionic liquids with cations which are derivatives of piperidinium or pyrrolidinium (six and five member rings, respectively) is similar to that of R_4N^+. Fig. 2 compares the typical steady state cyclic voltammograms of graphite electrodes (no matter which type) in MPPpTFSI with and without LiTFSI. In the absence of the Li salt, the voltammogram reflects irreversible cathodic reactions below 1 V. The reduction of the MPPp cation is expected to occur around 0 V (Li/Li$^+$), however, intercalation of the MPPp cations into graphite can occur at potentials around 0.5 V vs. Li/Li$^+$ [19,20]. Thereby, the cathodic peaks in the 0.8–0.2 V (Li/Li$^+$) range should be attributed to the irreversible reduction of TFSI anions, and insertion of MPPp cations, which occurs in the absence of electrode passivation. It should be noted that when the cations are derivatives of imidazolium, their reduction becomes the dominant cathodic process in these systems, below 1 V (Li/Li$^+$). As seen in Fig. 2, when the MPP_pTFSI solution contains LiTFSI, the graphite electrodes behave completely differently. They become passivated and the only relevant cathodic reaction at steady state is reversible Li intercalation/deintercalation. As we demonstrated recently [19,20], the scenario of the passivation of

graphite electrodes in these systems depends very strongly on the source and morphology of the graphite particles. For natural graphite flakes (the active mass relevant to Fig. 2) with relatively smooth edge planes, passivation is reached during a first polarization of the electrode in a MPP_pTFSI/LiTFSI solution. For synthetic graphite flakes whose edge planes are very rough, the electrodes have to undergo several repeated CV cycles in order to reach passivation, after which Li insertion–deinsertion becomes the cathodic process. For the synthetic graphite electrodes comprising particles with rough edge planes, the first cathodic polarization and the first few CV cycles involve co-intercalation of the IL cation (in the absence of good passivation).

As shown by several groups, it is possible to obtain reversible behavior of both graphite and Li electrodes in a wide variety of IL solutions by the use of active additives in solutions (e.g., vinylene carbonate) that react predominantly on the active electrode surface, thus forming passivating surface films [21,22]. Preliminary studies of the surface chemistry of active electrodes in LiTFSI solutions were carried out with lithium samples, prepared *in situ* in TFSI solutions, based on ethers. Ether solvents such as dimethyl ether (DME) or 1–3 dioxolane (DOL) are much less reactive than TFSI ions, and thus their solutions can serve as good probes for the study of the surface species formed by TFSI reduction (in the presence of Li ions) [23].

Fig. 3a shows an FTIR spectrum measured for a Li surface prepared in an ethereal LiTFSI solution, and Fig. 3b shows the XPS data related to a similar sample. The spectrum in Fig. 3a shows typical IR peaks of C—F, S=O and S—O groups, as indicated (around 1250, 1150–1100 and 1100–1000 cm^{-1}, respectively). Fig. 3b shows data dedicated to F, C, S and N, which indicate the formation of surface LiF (F_{1S} peak at 625 eV), $-CF_3$ and/or Li_xCF_y groups (F_{1S} peak at 689 eV and C_{1S} peak around 289–290 eV), nitrogen containing surface species (e.g., $Li_2NSO_2CF_3$), N_{1S} peak around 400 eV), and various sulfur species containing S=O and/or S—O bonds (S_{2P} peaks between 168 and 172 eV). These studies (coherent data from FTIR and XPS measurements) demonstrate that the reduction of TFSI ions in the presence of lithium ions can form a variety of passivating agents, all of which are insoluble, ionic lithium compounds (LiF, $Li_2NSO_2CF_3$, Li_xSO_y, $Li_xSO_2CF_3$ and Li_xCF_y). Note that in the absence of Li ions, e.g., in tetraalkyl ammonium salt solutions, all alkyl carbonate solvents are reduced on carbon or non-active metal electrodes to $ROCO_2^-$ species at potentials around 1 V vs. Li/Li^+ [17] (somewhat similar to the behavior of imidazolium-based IL solutions).

The message from these studies is that it is possible to use ILs in Li ion battery systems containing graphite, or even Li anodes, by controlling the electrodes passivation. This can be achieved by a good choice of Li salts and additives. Another important aspect of the use of ILs in Li batteries is their possible contribution to enhanced safety. There are questions regarding the use of ILs as the main body of the electrolyte solutions in Li-ion batteries, related to the still too high cost and to the high viscosity, which means a too slow rate capability at low temperatures. However, it may be possible to use ILs as additives to standard solutions. As was clearly demonstrated, [24] alkyl carbonates/$LiPF_6$ solutions by themselves are red-ox couples in which the PF_6^- anion oxidizes the alkyl carbonates at elevated temperatures in exothermal reactions. Reactions of lithiated carbon with PF_6^- and alkyl carbonates (the solution components are reduced), as well as reactions of transition metal oxides with solvent molecules (the latter are oxidized) may also lead too thermal runaway at elevated temperatures [25,26]. We examined the possibility of using ILs based on pyrrolydinium derivatives with different anions as thermal stabilizer additives (10% in standard EC-DMC/$LiPF_6$ 1 M solutions). ILs based on pyrrolydinium derivatives demonstrate wide electrochemical windows and can be suitable for use with lithium and lithiated graphite electrodes. The anions chosen were TFSI ($N(SO_2CF_3)_2^-$), FAP ($PF_3(CF_5)_3^-$), and BOB ($BC_4O_8^-$). We cannot demonstrate pronounced advantages of the presence of IL additives for the thermal stability of Li and Li-graphite in solutions. The presence of BMPBOB IL in solutions shows indeed a positive effect regarding the stabilization of Li and lithiated graphite in solutions at a wide temperature range. However, this is due to the BOB anion [27], and thus the same effect can be obtained by the presence of LiBOB, which is much cheaper and easier to use. Moreover, the BOB anion limits the anodic stability of both standard solutions and ILs due to its oxidation, which occurs below 4.5 V (Li/Li^+).

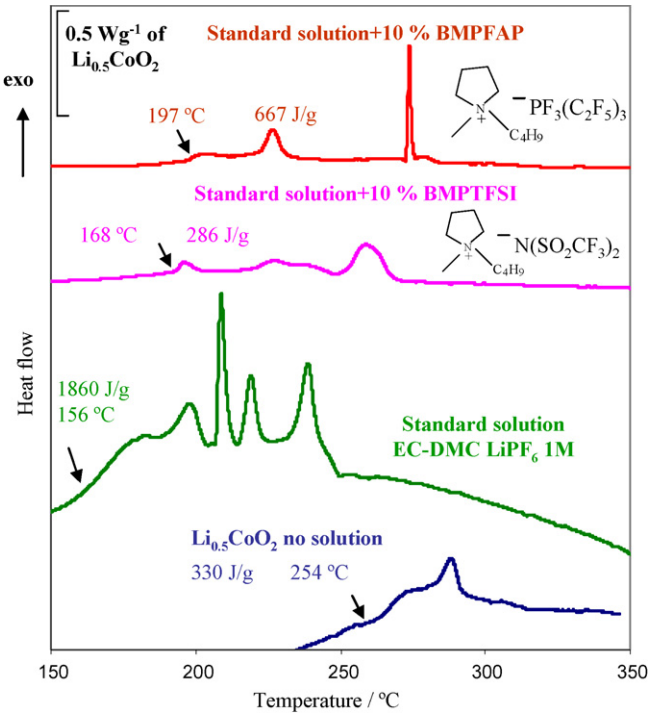

Fig. 4. DSC curve measured with $Li_{0.5}CoO_2$ in contact with standard EC-DMC/$LiPF_6$ 1 M solutions and standard solutions containing 10% ILs (by volume): N-butyl, methyl pyrrolidinium (BMP) TFSI and BMP-$PF_3(C_2F_5)_3$ (FAP), as indicated. The DSC curve of $Li_{0.5}CoO_2$ is also presented for comparison. The onset temperatures of the exothermal reactions and the specific heat evolved throughout the entire thermal reactions measured are indicated.

Fig. 4 shows the results of DSC studies of delithiated lithium cobalt oxide cathode material ($Li_{0.5}CoO_2$) with various solutions. The thermal behavior of the neat material is presented as well for comparison. The DSC response of $Li_{0.5}CoO_2$ with standard EC-DMC/$LiPF_6$ 1 M solutions demonstrates the well-known pronounced thermal reactions between the delithiated cathode material and solution species starting around 150 °C with further remarkable heat evolution (see data in the figure). The presence of 10% of either BMPFAP or BMPTFSI reduces remarkably the thermal activity of these systems: the onset temperature of the thermal reactions increases and the heat evolution decreases due to the presence of the IL additives, as presented in Fig. 4. It should be noted that BMPFAP and BMPTFSI dissolve the relevant Li salts (LiFAP and LiTFSI). The solutions thus obtained demonstrate pronounced anodic stability (>5 V vs. Li/Li^+) and allow the efficient passivation of both Li and Li-C electrodes.

Further studies are required in order to understand the mechanisms in which the presence of these ILs as additives can attenuate the thermal reactivity of standard solutions, and for the

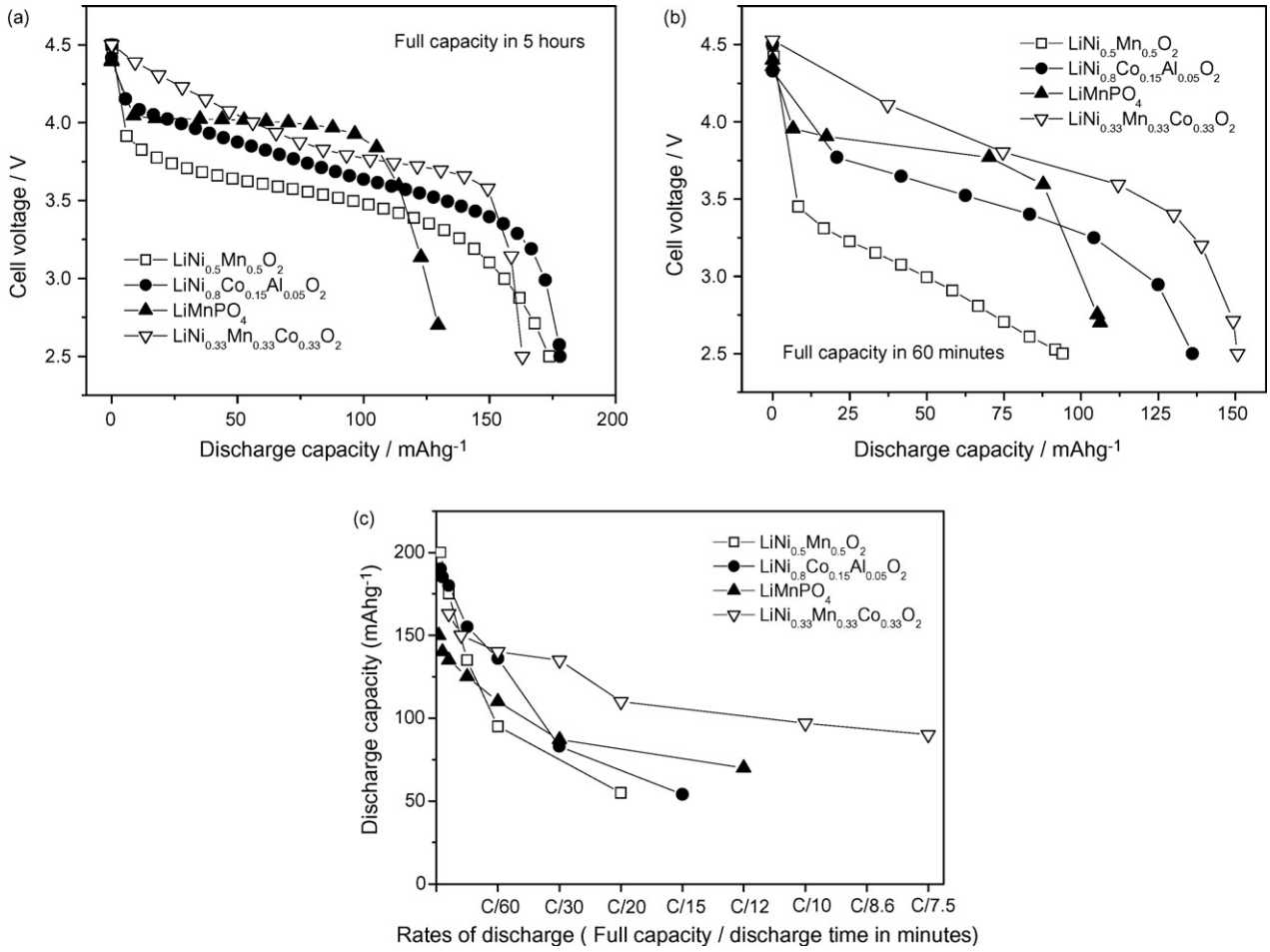

Fig. 5. Typical voltage profiles of $LiNi_{0.5}Mn_{0.5}O_2$, $LiNi_{0.8}Co_{01.5}Al_{0.05}O_2$, $LiNi_{0.33}Mn_{0.33}Co_{0.33}O_2$, and $LiMnPO_4$ electrodes measured galvanostatically at (a) C/5 (hours), (b) C/1 (hour) rates (30 °C) as indicated in standard EC-DMC/$LiPF_6$ solutions, and (c) discharge capacity vs. discharge rates of the four cathode materials (see Fig. 5(a) and (b)) during galvanostatic cycling at 30 °C in standard EC-DMC/$LiPF_6$ solutions between 4.5 and 2.5 V vs. Li/Li^+. The cycling protocol was constant current-constant voltage (for the charging steps), providing potentiostatic steps at 4.5 V during 2.5 h for cycling at C/5 and during 0.5 h for cycling at C/1 h.

optimization of compositions. However, these studies clearly show a possible important application of selected ILs as additives that may avoid dangerous thermal reactions in Li batteries.

3.2. On studies related to cathode materials

The theme of the present study was to compare the behavior of several advanced cathode materials in similar experiments in terms or capacity, capability, stability, and cycling, and to explore surface chemical aspects that influence the performance of these materials. The study reported herein was limited to standard electrolyte solutions (alkyl carbonates/$LiPF_6$)

Fig. 5a and b compares typical voltage profiles of composite electrodes comprising $LiNi_{0.5}Mn_{0.5}O_2$, $LiNi_{0.33}Mn_{0.33}Co_{0.33}O_2$, $LiNi_{0.8}Co_{0.15}Al_{0.05}O_2$, and $LiMnPO_4$ measured during galvanostatic cycling in EC-DMC/$LiPF_6$ solutions (30 °C) at C/5(hours) and C/1(hour) rates, (respectively). Fig. 5c compares the rate capability of these electrodes. The specific discharge (lithiation) capacity is plotted as a function of the rates (in terms of the duration in minutes of the discharge of the full capacity). The voltage limits for these cycling experiments were between 4.5–2.5 V vs. Li/Li^+). The application of this voltage range enabled the extraction of the maximal capacity of the layered material, without entering the problems of solution decomposition. The presentation of Fig. 5 allows the comparison of some basic properties of these systems:

1. The highest capacity, up to 200 mAh g^{-1}, can be extracted from $LiNi_{0.5}Mn_{0.5}O_2$. However, this material suffers from relatively low rate capability.
2. The fastest material (for reversible Li insertion/deinsersion) of the four systems presented in Fig. 5 is $LiNi_{0.33}Mn_{0.33}Co_{0.33}O_2$.
3. It was very significant to discover that the $LiMnPO_4$ electrodes could reach higher rate capabilities than both $LiNi_{0.5}Mn_{0.5}O_2$ and $LiNi_{0.8}Co_{0.15}Al_{0.05}O_2$ electrodes.
4. The voltage profiles of the layered nickel-based materials is sloping, while that of $LiMnPO_4$ is flat (due to the Li insertion into this material that involves first-order phase transition). The differences in the rate capabilities of the layered materials are discussed in the literature [28–30] in terms of the level of mixing between transition metal and Li cations in the relevant layers in the lattice. Further discussion on this matter is beyond the scope of this paper.

It is important, however, to discuss the possible difference in the rate capability of the layered and the olivine cathode materials. In recent years $LiFePO_4$ has become one of the most important cathode materials for Li-ion batteries [31]. Batteries containing $LiFePO_4$ cathodes are already commercial. Although the capacity of this material is 150–160 mAh g^{-1}, only slightly higher than that of commonly-used, $LiCoO_2$ and its operational voltage is relatively low (≈3.5 V compared to 3.9 V for $LiCoO_2$ vs. Li/Li^+), this mate-

rials seems very advantageous in terms of rate capability, safety features, and cost [32]. The high rate capability achievable with $LiFePO_4$ electrodes which is higher than that obtained with some layered cathode materials (Li_xMO_y, M=Ni, Co), is apparently surprising because both the ionic (Li^+ transport) and the electronic conductivities of the olivine materials are very low. The high rate capability achievable with these electrodes is due to the nano-$LiFePO_4$ material used that can be relatively easily synthesized and which particles are covered by electronically-conducting phases (e.g., carbon, iron phosphides [33]). As a cathode material with nano-size particles, the diffusion length for Li ions is sufficiently small to allow overall rapid enough Li-ion transport (despite the fact that it is one dimensional). The nano-size also facilitates electron tunneling from the current collector through the outer conductive coverage of the particles to the red-ox sites in the active mass. Our recent studies with $LiFePO_4$ electrodes [34] revealed that this material is much less reactive towards solution species in standard electrolytes compared with all other commonly-used cathode materials, e.g., $LiCoO_2$, $LiNiO_2$, $LiMn_2O_4$, V_2O_5. The oxygen atoms of $LiFePO_4$ are less basic and nucleophilic than the oxygen atoms of most lithiated transition metal oxides. This relatively low surface reactivity of $LiFePO_4$ enables its extensive use as a nano-material in cathodes, which allows the impressive rate capability that can be obtained. This low surface reactivity is in line with the high thermal stability of $LiFePO_4$ compared to other cathode materials [35]. In contrast, cathode materials such as $LiCoO_2$ and $LiNiO_2$ are very reactive with solution species [36]. Thereby, it seems irrelevant to use them as high surface area nano-materials in cathodes.

Fig. 6a and b compares FTIR spectra measured from pristine and aged $LiNi_{0.5}Mn_{0.5}O_2$ (Fig. 6a) and $LiMnPO_4$ (Fig. 6b) powders. The IR spectrum of pristine $LiNi_{0.5}Mn_{0.5}O_2$ shows, as expected, Li_2CO_3 peaks (indicated) due to reactions of the basic surface oxygen anions with CO_2. The spectrum of a $LiNi_{0.5}Mn_{0.5}O_2$ powder aged during several weeks in an EC-DMC/$LiPF_6$ solution is very rich in IR peaks, including carbonyl peaks around 1700–1800 cm^{-1}, which cannot belong to the residual solution. As discussed previously [37], such IR spectra reflect the formation of polycarbonate and metal alkyl carbonate ($ROCO_2M$, M=Li, Ni or Mn).

Our ongoing studies of all kinds of lithiated transition metal oxides: $LiCoO_2$. $LiNiO_2$, $Li[NiMn]O_2$, $Li[NiMnCo]O_2$, etc., show systematically their pronounced surface reactivity towards solution species in standard electrolyte solutions [7,36,37]. In contrast to the above, the spectra of pristine and aged $LiMnPO_4$ presented also in Fig. 6b are nearly the same, demonstrating a relatively low surface activity for this material, in a similar manner as is the case for $LiFePO_4$. The $LiMnPO_4$ from HPL studied herein is indeed nano-material (particle size is several tens of nanometer), which enables its relatively good rate capability of these electrodes, as demonstrated in Fig. 5c. Our studies seem to indicate that despite the much higher red-ox voltage of this material, compared to that of $LiFePO_4$ (0.6–0.7 V higher), it also demonstrates the relatively low surface reactivity of olivine compounds (due to the low basicity and nucleophilicity of the oxygen anions). Therefore, it is indeed relevant and possible to work with the nanoparticles of this material in standard electrolyte solutions, and hence, overcome the bad transport properties (electronic and ionic) of this material. While the $LiNi_{0.5}Mn_{0.5}O_2$ and $LiNi_{0.33}Mn_{0.33}Co_{0.33}O_2$ layered material studied in this work are indeed surface reactive, they develop impressive stability in standard electrolyte solutions, even at elevated temperatures. The surface chemistry and stability of $LiNi_{0.5}Mn_{1.5}O_4$ spinel and layered $LiNi_{0.5}Mn_{0.5}O_2$ in standard solutions at elevated temperatures was demonstrated and discussed previously [7,37]. The surface chemistry of $LiNi_{0.33}Mn_{0.33}Co_{0.33}O_2$ and $LiNi_{0.4}Mn_{0.4}Co_{0.2}O_2$ electrodes in standard solutions, studied by FTIR and XPS spectroscopy, is very similar to that of the

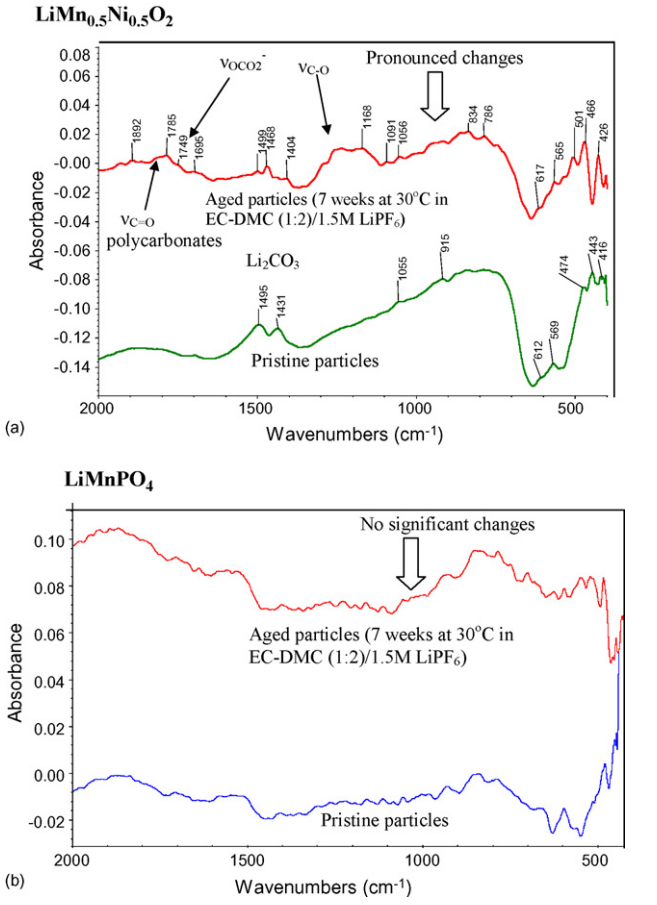

Fig. 6. FTIR spectra measured in diffuse reflectance mode for the pristine and aged (a) $LiNi_{0.5}Mn_{0.5}O_2$, and (b) $LiMnPO_4$ powders. Aging was carried out at 30 °C in standard EC-DMC/$LiPF_6$ solutions.

$Li[NiMn]O_2$ layered and spinel materials studied previously. FTIR spectra measured from aged $Li[NiMnCo]O_2$ particles are very similar to those presented in Fig. 6 for aged $LiNi_{0.5}Mn_{0.5}O_2$ particles. They reflect the formation of organic species such as polycarbonates and $ROCO_2M$. The former may be formed by the surface-induced polymerization of EC, and the latter may be a product of the nucleophilic attack of surface oxygen anions on alkyl carbonate molecules. The relevant XPS data related to C_{1s} are in line with the FTIR measurements, reflecting the formation of surface organic compounds that contain C—O and $—CO_2^-$ groups. The F_{1s} spectra indicate the formation of surface fluorides (may include both LiF and transition metal fluorides). These species can be formed by acid-base reactions with trace HF. Highly interesting is the finding that XPS data from aged particles reflect pronounced changes in the stoichiometry of the transition metal cations near the surface. From the XPS measurements it seems that Mn and Co diminish near the surface, i.e., the Ni/Co and Ni/Mn ratios measured after aging in solutions, become much greater than 1). This finding is very interesting because in previous studies we found that $LiNiO_2$ is much more surface active in standard electrolyte solutions than $LiCoO_2$ and $LiMn_2O_4$ [36]. Hence, we can speculate that the oxygen bound to nickel may be more reactive (basic and/or nucleophilic) than oxygen bound to Co or Mn. Therefore, their surface reactions may form species such as NiF_2, NiF_3, and $ROCO_2Ni$ that cover the surface, thus masking the active mass (lower intensity of the Mn and Co XPS peaks related to aged electrodes), but leaving Ni ions on the surface, included in the surface species formed by interactions between the active mass and solution species.

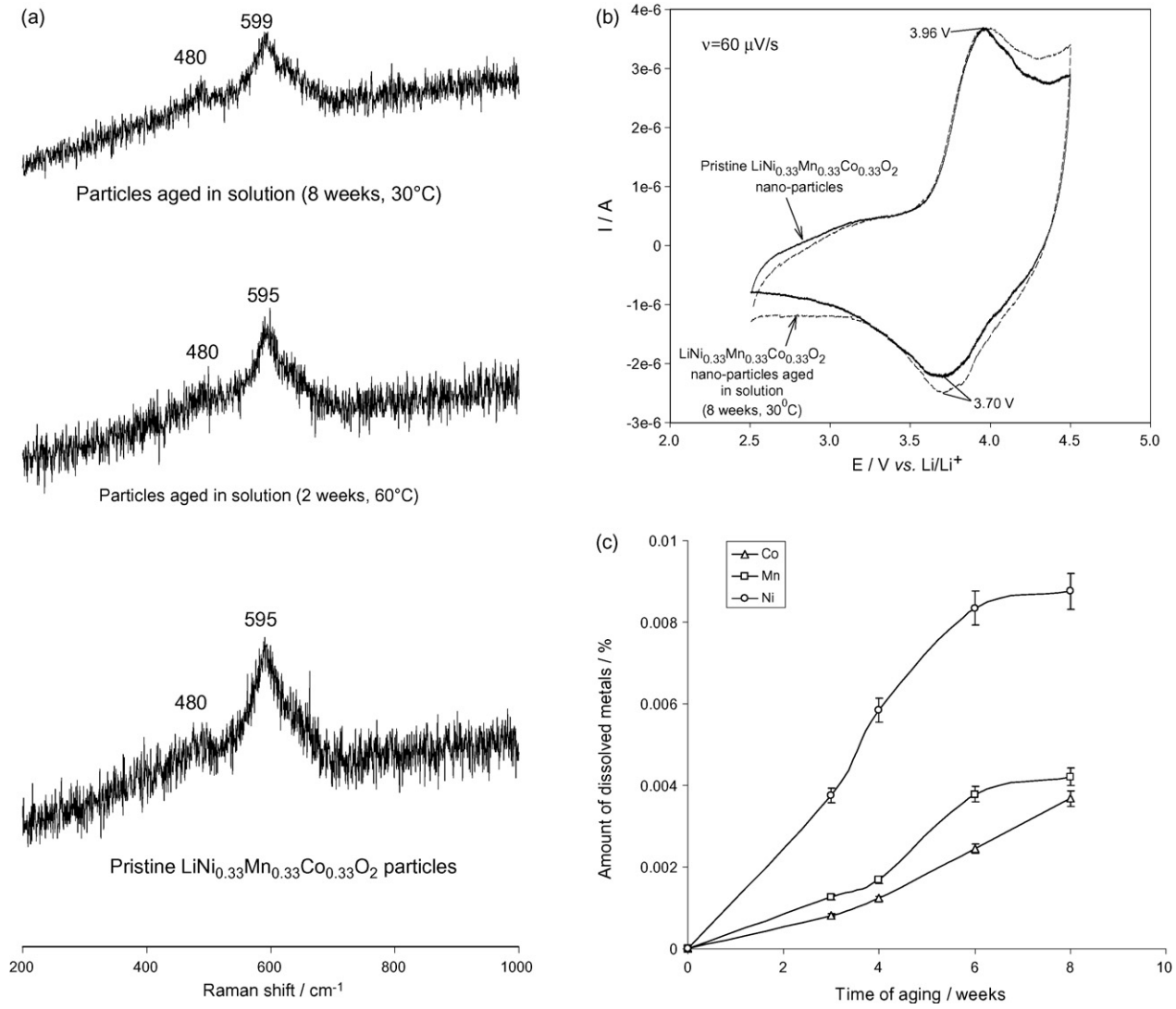

Fig. 7. (a) Raman spectra measured from pristine and aged nano $LiNi_{0.33}Mn_{0.33}Co_{0.33}O_2$, as indicated. Aging was carried out in a glove box in standard EC-DMC/$LiPF_6$ solutions. One measurement was carried out after aging at 30 °C during 8 weeks, and another measurement was conducted after aging at 60 °C during 2 weeks. (b) Steady state cyclic voltammograms measured with pristine and aged (8 weeks at 30 °C) $LiNi_{0.33}Mn_{0.33}Co_{0.33}O_2$ electrodes in EC-DMC/$LiPF_6$ standard solutions at scan rate 60 $\mu V\,s^{-1}$. These electrodes contained no binder and carbon additives and were prepared by embedding (pressure) the active mass onto aluminum current collector. (c) The percentage of Ni, Mn and Co dissolution from $LiNi_{0.33}Mn_{0.33}Co_{0.33}O_2$ powder into EC-DMC 1:2/1.5 M $LiPF_6$, in a glove box, during 8 weeks at 30 °C (magnetic stirring), as indicated. The concentrations of the transition metal cations in the solution were measured by ICP.

We described previously the impressive stability of spinel $LiMn_{1.5}Ni_{0.5}O_4$ and layered $LiMn_{0.5}Ni_{0.5}O_2$ electrodes in standard solutions, even at elevated temperatures, which enabled the cycling of both types of electrodes at 60 °C with very minor capacity fading [7,37]. $LiMn_{0.33}Mn_{0.33}Co_{0.33}O_2$ electrodes also demonstrate a similar impressive stability. Some relevant data are presented in Fig. 7a–c. Fig. 7a compares the Raman spectrum of pristine $LiNi_{0.33}Mn_{0.33}Co_{0.33}O_2$ to that of the same material aged at 30 °C and 60 °C in EC-DMC/$LiPF_6$ solutions. The three spectra are very similar and reflect no change in this active mass upon aging in solution. Fig. 7b demonstrates the stability of these electrodes upon aging, by comparing the slow scan-rate CVs of pristine and aged electrodes (8 weeks, 30 °C) measured in EC-DMC/$LiPF_6$ solutions. We measured the possible dissolution of transition metal cations from $LiNi_{0.33}Mn_{0.33}Co_{0.33}O_2$ powder into EC-DMC 1:2/1.5 M $LiPF_6$ solutions in experiments containing a high ratio between the solution volume and the active mass (i.e., no solubility limitation due to saturation). Typical results can be seen in Fig. 7c. In general the dissolution rate of Mn is more than twice as high as that of Ni and Co, which is nearly similar. The total amount of dissolved Mn during 8 weeks of aging is lower than 0.01%. As seen in this figure, the dissolution of the transition metal cations ceases after a few weeks, and hence, the amount of dissolved metal cations in solution stabilizes much before any possible saturation is reached. These results seem to indicate that while transition metal dissolution from this material to the electrolyte solutions is possible, and occurs to some extent at 30°C, the active mass probably develops passivation due to the above-described surface chemistry that forms a protective layer comprising insoluble products (metal fluorides, metal alkyl carbonates, polycarbonate). Interesting questions are still unanswered relating to the surface chemistry of the $LiNi_{0.8}Co_{0.15}Al_{0.05}O_2$ material and the possible role of aluminum in attenuating the relatively high surface reactivity of $Li[NiCo]O_2$ cathode materials. The effect of the electrodes' potential and the state of lithiation on the aging behavior and surface chemistry of the materials discussed herein is also an unanswered question.

Finally, the practical use of all of these materials depends on their thermal stability and to what extent it can be controlled by the

use of new electrolyte systems (e.g., ionic liquids) and/or by the use of additives to the standard electrolyte solutions. Further studies of the surface chemistry of these systems, aiming at answering the above open questions are underway.

4. Conclusions

We demonstrated the possibility of using ILs based on cyclic, quaternary ammonium cations in Li-ion battery systems, thus gaining several possible advantages, i.e., wide electrochemical windows that allow the operation of 5 V Li batteries (e.g., using $LiNi_{0.5}Mn_{1.5}O_4$ cathodes), achieving the good stabilization of graphite electrodes, and improving the safety features, even when used as additives. The nature of the anionic counterpart is highly important. When the anions were $N(SO_2CF_3)_2^-$ (TFSI) and $PF_3(C_2F_5)_3^-$ (FAP), the presence of 10% of ILs based on N-butyl-methyl pyrrolidinium (with these two anions) in standard electrolyte solutions, improved the thermal stability of delithiated $Li_{0.5}CoO_2$. TFSI-based ILs with cycling quaternary ammonium cations (e.g., N-butyl, methyl pyrrolidinium or piperidinium) demonstrated very impressive anodic stability, >5.5 V vs. Li/Li^+. In the presence of Li ions, the reduction of the TFSI anion by lithium or lithiated graphite forms passivating surface species that may include LiF, $Li_2NSO_2CF_3$, Li_xSO_y, Li_xCF_y, and $Li_xSO_yCF_z$ moieties. Hence, both Li and Li-graphite electrodes work well in LiTFSI solutions of these TFSI-quaternary ammonium-based ILs.

Several aspects related to the performance of important cathode materials were also dealt with in this work. The lithiated transition metal oxides, such as spinel $Li[MnNi]O_4$ and layered $Li[MnNi]O_2$ or $Li[MnNiCo]O_2$ develop a similar surface chemistry in standard solutions, which relate to the basicity and nucleophilicity of their surface oxygen atoms. We have indications that the presence of Ni in all of these compounds enhances the nucleophilicity of the surface oxygen. Electrodes based on all of these materials seem to reach very good passivation in standard $LiPF_6$/alkyl carbonate-based solutions, due to the formation of surface species such as LiF, MF_x, $ROCO_2Li$, $ROCO_2M$, and polycarbonates. However, it is doubtful whether it is relevant to use them as nano-materials and hence gain high rate capability, due to their pronounced surface reactivity. In contrast, $LiMnPO_4$ can be used as a nano-material in cathodes, thus demonstrating impressive rate capability, despite poor intrinsic ionic and electronic transport properties. This is due to the much lower surface reactivity of the olivine compounds (e.g., $LiFePO_4$, $LiMnPO_4$) compared to the transition metal oxides.

Acknowledgement

Partial support for this work was obtained from the ISF, Israel Science Foundation.

References

[1] D. Aurbach, Y. Gofer, in: D. Aurbach (Ed.), Nonaqueous Electrochemistry, Marcel Dekker, N.Y, 1999, pp. 137–212.
[2] E. Peled, in: J.P. Gabano (Ed.), Li Batteries, Accdemic Press, London and N.Y., 1983, Chapter 3.
[3] M. Moshkovich, M. Cojocaru, H.E. Gottlieb, D. Aurbach, J. Electroanal. Chem. 497 (2001) 84–96.
[4] M. Morita, T. Shibata, N. Yoshimoto, M. Ishikawa, J. Power Sources 119-121 (2003) 784–788.
[5] D. Aurbach, M.D. Levi, E. Levi, H. Teller, B. Markovsky, G. Salitra, U. Heider, L. Heider, J. Electrochem. Soc. 145 (1998) 3024–3034.
[6] A. Blyr, C. Sigala, G. Amatucci, D. Guyomard, Y. Chabre, J.-M. Tarascon, J. Electrochem. Soc. 145 (1998) 194–209.
[7] Y. Talyossef, B. Markovsky, R. Lavi, G. Salitra, D. Aurbach, D. Kovacheva, M. Gorova, E. Zhecheva, R. Stoyanova, J. Electrochem. Soc. 154 (2007) A682–A691.
[8] S. Komaba, N. Kumagai, Y. Kataoka, Electrochim. Acta 47 (2002) 1229–1239.
[9] E. Markevich, G. Salitra, D. Aurbach, Electrochem. Commun. 7 (2005) 1298–1304.
[10] B. Markovsky, A. Rodkin, G. Salitra, Y. Talyosef, D. Aurbach, H.-J. Kim, J. Electrochem. Soc. 151 (2004) A1068–A1076.
[11] D. Kovacheva, H. Gadjov, K. Petrov, S. Mandal, M.G. Lazarraga, L. Pascual, J.M. Amarilla, R.M. Rojas, P. Herrero, J.M. Rojo, J. Mater. Chem. 12 (2002) 1184–1188.
[12] J.S. Gnanaraj, Y.S. Cohen, M.D. Levi, D. Aurbach, J. Electroanal. Chem. 516 (2001) 89–102.
[13] D. Aurbach, J. Electrochem. Soc. 136 (1989), 906, 1606 and 1611.
[14] E. Markevich, V. Baranchugov, D. Aurbach, Electrochem. Commun. 8 (2006) 1331–1334.
[15] M.D. Levi, G. Salitra, B. Markovsky, H. Teller, D. Aurbach, U. Heider, L. Heider, J. Electrochem. Soc. 146 (1999) 1279–1289.
[16] B. Markovsky, Y. Talyossef, G. Salitra, D. Aurbach, H.-J. Kim, S. Choi, Electrochem. Commun. 6 (2004) 821–826.
[17] D. Aurbach, H. Gottlieb, Electrochim. Acta 34 (1989) 141–156.
[18] M.C. Kroon, W. Buijs, C.J. Peters, G.-J. Witkamp, Green Chem. 8 (2006) 241–245.
[19] E. Markevich, V. Baranchugov, G. Salitra, D. Aurbach, M.A. Schmidt, J. Electrochem. Soc. 155 (2008) A132–A137.
[20] V. Baranchugov, E. Markevich, G. Salitra, D. Aurbach, G. Semrau, M.A. Schmidt, J. Electrochem. Soc. 155 (2008) A217–A227.
[21] H. Zheng, K. Jiang, T. Abe, Z. Ogumi, Carbon 44 (2006) 203–210.
[22] M. Holzapfel, C. Jost, A. Prodi-Schwab, F. Krumeich, A. Würsig, H. Buqa, P. Novák, Carbon 43 (2005) 1488–1498.
[23] D. Aurbach, O. Chusid, I. Weissman, P. Dan, Electrochim. Acta 41 (1996) 747–760.
[24] J.S. Gnanaraj, E. Zinigrad, L. Asraf, H.E. Gottlieb, M. Sprecher, M. Schmidt, W. Geissler, D. Aurbach, J. Electrochem. Soc. 150 (2003) A1533–A1537.
[25] Y. Wang, K. Zaghib, A. Guerfi, F.F.C. Bazito, R.M. Torresi, J.R. Dahn, Electrochim. Acta 52 (2007) 6346–6352.
[26] M. Taggougui, M. Diaw, B. Carré, P. Willmann, D. Lemordant, Electrochim. Acta 53 (2008) 5496–5502.
[27] K. Xu, S. Zhang, B.A. Poese, T.R. Jow, Electrochem. Solid-State Lett. 5 (2002) A259–A262.
[28] T. Ohzuku, R.J. Brodd, J. Power Sources 174 (2007) 449–456.
[29] P. Reale, D. Privitera, S. Panero, B. Scrosati, Solid State Ionics 178 (2007) 1390–1397.
[30] E. Zecheva, R. Stoyanova, R. Alcántara, P. Lavela, J.L. Tirado, J. Power Sources 174 (2007) 519–523.
[31] D.-H. Kim, J. Kim, Electrochem. Solid-State Lett. 9 (2006) A439–A442.
[32] S.Y. Chung, J.T. Bloking, Y.-M. Chiang, Nat. Mater. 1 (2002) 123–128.
[33] P.S. Herle, B. Ellis, N. Coombs, L.F. Nazar, Nat. Mater. 3 (2004) 147–152.
[34] M. Koltypin, D. Aurbach, L.F. Nazar, B. Ellis, Electrochem. Solid-State Lett. 10 (2007) A40–A44.
[35] J. Jiang, J.R. Dahn, Electrochem. Commun. 6 (2004) 39–43.
[36] D. Aurbach, K. Gamolsky, B. Markovsky, G. Salitra, Y. Gofer, U. Heider, R. Oesten, M. Schmidt, J. Electrochem. Soc. 147 (2000) 1322–1331.
[37] B. Markovsky, D. Kovacheva, Y. Talyosef, M. Gorova, J. Grinblat, D. Aurbach, Electrochem. Solid-State Lett. 9 (2006) A449–A453.